

SIMULATION RESULTS FOR AN INNOVATIVE ANTI-MULTIPATH DIGITAL RECEIVER

J. H. PAINTER

**National Aeronautics and Space Administration
Langley Research Center
Hampton, VA.**

L. R. WILSON¹

**LTV Aerospace Corp.
Hampton, VA.**

Summary Simulation results are presented for the error rate performance of the recursive digital MAP detector for known M-ary signals in multiplicative and additive Gaussian noise. The structure of the digital simulation of the innovative receiver, operating in a multipath environment, is generally described. Specific results are given for a quaternary signal, of the type used in air-ground data links, with 2500 symbol per second transmission rate. Plots of detection error rate versus additive signal to noise ratio are given, with multipath interference strength as a parameter. For comparison, the error rates of conventional coherent and noncoherent digital MAP detectors are simultaneously simulated and graphed. It is shown that with non-zero multiplicative noise, the error rates of the conventional detectors saturate at an irreducible level as additive signal to noise ratio increases. The error rate for the innovative detector continues to decrease rapidly with increasing additive signal to noise ratio. In the absence of multiplicative interference, the conventional coherent detector and the innovative detector are shown to exhibit identical performance.

Introduction A recent paper² describes a recursive digital receiver for known M-ary signals in a multipath environment. The transmission medium is characterized by white additive and low-pass multiplicative Gaussian perturbations of the signal. The receiver is optimum in the sense of minimum probability of error.

¹ Mr. Wilson's work was supported by the National Aeronautics and Space Administration under Contract No. NAS1-10900.

² J.H. Painter and S.C. Gupta, "Recursive Ideal Observer Detection of Known M-ary Signals in Multiplicative and Additive Gaussian Noise," IEEE TRANS. ON COMM., vol. COM-21, no. 8, Aug. 1973.

Figure 1. is the receiver structure. The outputs of the M parallel independent channels are proportional, respectively, to the A Posteriori probabilities of transmission, given the received data, for each of the M signals. When the output of the J th channel is largest, it is decided that the J th signal was received. After each decision, all the Kalman filters are re-initialized to the last values in the “correct” filter. Succeeding signals are detected in this “decision-directed” mode.

The receiver thus implemented is adaptive in the sense that it estimates the multiplicative disturbance. The first and second order statistics of the multiplicative process and the power level of the additive noise must be fed to the receiver. Since these processes are generally nonstationary, the receiver must be further adapted to changing statistics. Methods for estimating the statistical parameters in real time are the subject of present work by the authors and will be treated in a future paper.

In the present paper are documented the first results of a computer simulation of the optimum receiver, in which the receiver has precise knowledge of the mean and covariance of the multiplicative process and of the variance of the additive noise. These results give the lower bound on error rate for practical receivers in which the statistical parameters must be continuously estimated.

In this simulation, a well balanced sequence of 0's and 1's is randomly generated and differentially encoded into a quaternary alphabet. The signal is passed through the simulated channel and processed by the optimum receiver. Since the simulation “knows” which character was transmitted, the receiver errors can be detected and recorded. Care is taken that the signal sequence be longer than a few correlation times of the multiplicative noise. A number of statistically independent simulation runs is used so that the results are statistically significant.

The graphical results presented are plots of detection error rate (probability of error per bit) versus the ratio of unperturbed signal power to additive noise power (additive SNR, hereafter). Families of curves are plotted, with “multiplicative SNR” as parameter.

For comparison purposes, error rate curves are simultaneously obtained for the conventional coherent and incoherent digital MAP receivers (matched filters, essentially). The latter are designed to be optimum in the presence of the additive white noise, alone.

The inspiration for this work was the problem of optimizing air-ground communications in the presence of ground reflection and scattering. The mathematical model used below is thus somewhat predisposed to this particular context. However, the results are clearly extendable to other situations.

Design of the Simulation Inasmuch as the emphasis in this paper is on receiver performance, a simplified channel model is adopted, without, however, impairing the equivalence of the simulation to physical reality. The transmitted signal is taken in a quite general form as

$$\sigma(t,m) = A(t,m) \exp \{j [\omega t + \phi(t,m)]\} \quad (1)$$

where $A(\)$ and $\phi(\)$ are real, with $0 \leq A(\)$. The index, m , denotes which distinct waveform, of M possible, is transmitted. ω is the radian carrier frequency.

The received signal is then defined to be

$$\zeta(t,m) = \chi(t) \sigma(t,m) + v(t) \quad (2)$$

where $\chi(t)$ is a lowpass complex non-zero-mean Gaussian process, and $v(t)$ is white, zero-mean, Gaussian, and independent of $\chi(t)$. Note that in connecting equation (2) to the multipath situation, overall transmission delays are disregarded. Differential path delays are reflected in the behavior of $\chi(t)$. This is a common formulation for the non-frequency-selective fading channel.^{3 4}

Physically, the received signal is taken as the real part of $\zeta(t,m)$. Thus, define

$$z(t,m) = \text{Re}\{\zeta(t,m)\} \quad (3)$$

Since the optimum detector of reference 1 is coherent, the Kalman filters may be more easily implemented by first demodulating $z(t,m)$ in quadrature. Define

$$z_i(t,m) = 2 z(t,m) \cos[\omega t + \phi_0(t)] \quad (4)$$

$$z_q(t,m) = -2 z(t,m) \sin[\omega t + \phi_0(t)]$$

The term, $\phi_0(t)$, represents any residual phase disturbance which may be present as a result of deriving the phase references for the carrier demodulators.

A continuous-time received data vector may now be defined as

$$\underline{z}(t,m) = H_0(t) \{H(t,m) \underline{x}(t) + \underline{n}(t)\} \quad (5)$$

³ L.A. Frasco and H.D. Goldfein, "Signal Design for Aeronautical Channels," IEEE TRANS. ON COMM., vol. COM-21, no. 5, pp. 534-547, May, 1973.

⁴ J.H. Painter, S.C. Gupta, and L.R. Wilson, "Multipath Modeling for Aeronautical Communications," IEEE TRANS. ON COMM., vol. COM-21, no. 5, pp. 658-662, May 1973.

where

$$\underline{z}(t,m) = \begin{bmatrix} z_i(t,m) \\ z_q(t,m) \end{bmatrix} ; \underline{x}(t) = \begin{bmatrix} x_i(t) \\ x_q(t) \end{bmatrix} ; \underline{n}(t) = \begin{bmatrix} n_i(t) \\ n_q(t) \end{bmatrix} \quad (6)$$

$$H_0(t) = \begin{bmatrix} \cos \phi_0(t) & \sin \phi_0(t) \\ -\sin \phi_0(t) & \cos \phi_0(t) \end{bmatrix} ; H(t,m) = A(t,m) \begin{bmatrix} \cos \phi(t,m) & -\sin \phi(t,m) \\ \sin \phi(t,m) & \cos \phi(t,m) \end{bmatrix}$$

In equation (6), $x_i(t)$ and $x_q(t)$ are the real and imaginary parts of the multiplicative $\chi(t)$. Likewise, $n_i(t)$ and $n_q(t)$ are the real and imaginary parts of $v(t)$ and are white, zero-mean, independent, and Gaussian. It can be seen that in the case of a perfect phase reference, the “demodulation matrix”, $H_0(t)$, is the unit 2X2 matrix. In the derivation of the optimum detector, a perfect phase reference was assumed. In the sequel will be considered the case for non-zero $\phi_0(t)$.

The continuous data is uniformly sampled at a rate of K samples per signal character. The discrete-time notation is formally identical to that above, with t replaced by a sample number, k . For example, $\underline{z}(t,m) \rightarrow \underline{z}(k,m)$, etc.

In the actual computation of $H(k,m)$, t is functionally replaced by

$$t = t_k = \left(\frac{k-1}{K} - \text{Int} \left\{ \frac{k-1}{K} \right\} \right) T ; \forall k = 1, 2, \dots \quad (7)$$

where $\text{Int}\{ \}$ denotes “integer part”, and T is the period of each signal character. This scheme “centers” the K samples in the signal intervals of length T so that none of the samples fall at ends of intervals, which are the signal transition times.

Figure 2. is a block diagram of the simulation. A pre-existing program is used to generate the mean and covariance of $\underline{x}(k)$, from scalar Kirchoff solutions of the very rough or slightly rough surface propagation problem for arbitrary reflection geometries.⁵ The desired direct-path/multipath characteristics are obtained by manipulating the reflection geometry and the rough surface parameters.

The multipath statistics are used to drive the multipath process generator. In this paper, these statistics are also hard-wired to the optimum detector, bypassing the adaptive circuitry. The multipath process is represented in equation (6) as a 2-vector. However, the process generator may have a greater number of internal states if $\underline{x}(k)$ is required to

⁵ P. Beckmann and A. Spizzichino, “The Scattering of Electro-magnetic Waves from Rough Surfaces,” Pergamon Press, 1963.

possess a Markov property of order greater than unity. Here, for simplicity, the state dimension of the generator has been chosen as 2. This is equivalent to generating $x_i(t)$ or $x_q(t)$ from white noise passed through slowly time-varying single-tuned filters. Also, $x_i(j)$ and $x_q(k)$ have been taken as uncorrelated for all j,k . This is a reasonable assumption for reflecting surfaces which do not exhibit rms. slopes greater than, say, 15° .

The present results are for an aeronautical communication system of current interest.⁶ Thus, the message generator produces a digital sequence from a quaternary alphabet. The sequence is actually produced by differentially encoding a pseudo-random binary sequence of 0's and 1's. Because the quaternary characters are used to generate the signal modulation directly, the alphabet used is the set, $\{-2,-1,+1,+2\}$ rather than the set, $\{0,1,2,3\}$. Thus, rather than dealing with signal digits, $m \in \{0,1,2,3\}$, we deal with the digits, $q \in \{-2,-1,+1,+2\}$. The digits, q , are generated by the difference relation

$$q(N) = 3 b(N-1) + b(N) - 2 \quad (8)$$

where N is the digit number in the sequence, $b(\)$ is the binary digit, and $q(\)$ is the quaternary digit.

The binary digits are generated in such a manner that the 0's and 1's are equally likely and succeeding digits are independent. Under these conditions, it is not difficult to show that the resulting quaternary digits are also equally likely.

The signal envelope and phase functions used are (cf. (1) and (7))

$$\phi(k,q) = 0$$

$$A(k,q) = 1 + \sin \left[q(N) \frac{\pi t_k}{T} \right] \quad (9)$$

The signal thus formed is 100% amplitude modulated by half or full cycles of sine waves with plus or minus polarities. This signalling scheme is seen to have the characteristics of both PSK and FSK. It is known as MSK, for minimum shift keying.⁷

The multipath process, $\underline{x}(k)$, the modulation, $H(k,q)$, and the additive noise, $\underline{n}(k)$, are combined as per equation (5) to generate the required vector, $\underline{z}(k,q)$. In the event that

⁶ N.D. Steele, Jr., "The ARINC Plan for Implementation of Data Link for the Airlines," PROC. 1971 ANN. ASSMBY. MTG., Paper AS-298, The Radio Tech. Commission for Aeron., Wash. D.C., Nov. 17-18, 1971.

⁷ L.A. Frasco, "Signal Design for AEROSAT," ANN. REPT. JAN/JUNE 1972, Appndx. B, U. S. Dept. Transp. , Transp. Syst. Ctr. , Cambridge, Mass., Aug. 1972.

imperfect phase references are used for carrier demodulation, the matrix, $H_0(k)$, multiplies $\underline{z}(k,q)$.

The variance of each component of $\underline{n}(k)$ is set to some prescribed value, and subsequently varies in proportion to the square of the length of the direct path between transmitting and receiving antennas. This is required, since all signal levels are normalized to that signal strength which is observed at unit distance in the absence of multipath.

The simulated data process is fed in parallel to the inputs of the optimum detector and the conventional coherent and incoherent detectors. All three detectors process the total received vector, $\underline{Z}(K)$, which is the K -sample vector of the 2-vector process, $\underline{z}(k,q)$, taken during the basic signal symbol period.

All the detectors attempt to calculate the joint probability densities, $p(\underline{Z}(K),q)$, for each of the four possible values of q . However, each detector employs different assumptions concerning the received data. The optimum detector assumes a perfect phase reference, for which $\phi_0(k) = 0$. The coherent detector assumes a perfect phase reference and also no multipath, so that $\underline{x}(k) = (1,0)^T$. Thus, the coherent detector sees, essentially, only the in-phase component of the received data vector, that is, $z_i(k)$. The incoherent detector assumes no multipath and also that $\phi_0(k)$ is constant and is uniformly distributed over $[0,2\pi]$. Thus, the incoherent detector first forms the density, $p(\underline{Z}(K),q,\phi_0)$, and then averages it over ϕ_0 .

The resulting densities for the optimum detector and for the coherent detector are weighted Gaussian functions and are not difficult to implement. The resulting density for the incoherent detector is awkward, involving the modified Bessel function, $I_0(\)$. Although this latter detector would not likely be implemented in practice, it is still useful as a standard for comparison. Incidentally, the reason that the argument of $I_0(\)$ does not form the usual sufficient statistic for detection is that the four possible signals are not of equal energy.

All the detectors decide on that signal which gives the greatest joint density. Then the detected signal digits at the output of the three detectors are compared to the transmitted signal, and the errors are recorded. A fairly large number of simulation runs is taken over the same geometry with different initial randomization of the multipath generator. Each run is taken over five correlation times of the process, $\underline{x}(k)$, or for a number of signal digits equal to 1.5 times the inverse error rate, whichever gives a greater period of time. The mean, μ , of the error rate and the standard deviation, σ , are computed over all the runs. The results are not accepted for $\mu/\sigma < 1.0$.

The simulation program was written in FORTRAN 4.3 for the CDC-6600 system. The program contains approximately 900 instructions, requiring 52400₈ locations for compilation and 23400₈ locations for execution. The Central Processing Unit time required is approximately 140 seconds per 1000 signal symbols of data. Among the inputs to the program are included the following: polarization (horizontal or vertical); heights of receiving and transmitting antennas; initial ground range; initial additive noise power; aircraft velocity; terrain conductivity, dielectric constant, rms. height and slope; signal digit rate; number of samples per digit; number of digits per run; and number of runs per job.

Simulation Results The results are presented in the form of plots of error rate versus the additive SNR, with the multiplicative SNR (MPSNR) as parameter. Because of computer time and expense factors, the error rate range is limited to be from 1.0 to 10⁻⁴

The various SNR are defined as follows. In the absence of multipath, x_i(k) is unity and x_q(k) is zero, x_i(k) representing the direct path signal. The additive SNR is thus defined as

$$\text{SNR} = \frac{2}{\text{tr}[\text{cov}\{\underline{n}(k)\}]} = \frac{1}{v_n(k)} \quad (10)$$

where

$$[\text{cov}\{\underline{n}(k)\}] = E\{\underline{n}(k)\underline{n}^T(k)\} = v_n(k) \begin{bmatrix} 1 & 0 \\ 0 & 1 \end{bmatrix} \quad (11)$$

tr { } denotes "trace of a matrix" and [cov{ }] denotes the covariance matrix.

The SNR for the multiplicative noise is defined by

$$\begin{aligned} \text{MPSNR} &= \frac{\text{tr} [\text{cov}\{\underline{x}(k)\}]}{\text{tr} [\bar{\underline{x}}(k)\bar{\underline{x}}^T(k)]} \\ &= \frac{\text{cov}\{x_i(k)\} + \text{cov}\{x_q(k)\}}{\bar{x}_i^2(k) + \bar{x}_q^2(k)} \end{aligned} \quad (12)$$

where the upper bar denotes expectation.

For intuitive clarification, it should be noted that for no carrier modulation (A(k,m) = 1, φ(k,m) = 0) and no multiplicative noise, the quantity, SNR, defined in equation (10) is related to the ratio of carrier power to additive noise, CNR, on a per-sample basis, by

$$\text{SNR} = 2 \text{ CNR} \quad (13)$$

The intuitive definition for MPSNR is that, in the absence of signal modulation, it is the ratio of Gaussian process power due to multipath only, divided by specular carrier power. This second definition holds true whether the multipath is caused by a totally diffuse surface reflection or whether the surface reflection has some specular component.

In order to plot an error rate curve, it is necessary to vary SNR while holding MPSNR constant. It is also necessary to run the simulation for a sufficient number of signal digits to obtain the required statistical significance. Because the simulation is driven by actual vehicle flight trajectories over rough surfaces, the strength of the multipath and its correlation time are interdependent. Thus, in order to reduce simulation run times on the machine, it is necessary to run in an almost completely diffuse reflection environment. Even for these cases, the multipath correlation times and, hence, the bandwidths of the multipath process, vary over the ranges of MPSNR used. The performance of the optimum detector may change somewhat as the ratio of signal bandwidth to multipath bandwidth varies widely. The effect was observed in the following simulation results.

Figure 3., the first family of curves, gives the performance of the optimum detector alone, for values of MPSNR of -3 dB., -7 dB., -10 dB., and for no multiplicative noise, respectively. The transmission digit rate is 2500 symbols per second, with a sampling rate of 10 samples per symbol. The equivalent low-pass single-sided noise bandwidth for the multipath process varies from 211 Hz., at -3 dB., to 10.5 Hz., at -10 dB. A perfect phase reference is assumed for carrier demodulation.

It is seen that the detector performance Improves rapidly as the SNR increases, from the “pure guess” value of 0.75 to a roughly exponential decay. As expected, increasing multipath strength requires increased additive SNR to compensate. The dotted trace in the figure shows the -3 dB. results for a transmission rate of 250 symbols per second, all other parameters being equal.

Figure 4. compares the -3 dB. MPSNR results for the three detectors, at 2500 symbols per second rate, with 10 samples per symbol, and perfect demodulation phase. The expected saturation of the error rates for the two conventional detectors is apparent. Also shown is the performance of the three detectors for no multiplicative noise, at all. The dashed curve, representing the incoherent detector, converges to the solid curve, representing the other two detectors, for increasing SNR. Examination of the simulation records shows that the coherent detector and the optimum detector make precisely the same errors in this case. Thus, their performance for no multipath is identical.

Because the multiplicative process is low-pass, it is difficult to recover a phase-stable carrier component with which to demodulate the carrier. Figure 5. shows the -3 dB. MPSNR performance of the three detectors when the carrier demodulation phase term,

$\phi_0(k)$, is that which would be encountered with -3 dB. multipath and no filtering. It is seen that the optimum detector and the standard non-coherent detector perform just the same as with perfect phase. The standard coherent detector now performs at par with the non-coherent detector.

The second set of results on this graph is a comparison of the standard coherent detector and optimum detector for -13 dB. MPSNR. Although the coherent detector is not saturating for error rates of 10^{-4} or greater, its performance is still markedly poorer than that of the optimum detector, even for this small amount of multipath.

Conclusion The simulation has demonstrated the superior performance of an optimum detector, specifically adapted to a multipath channel in which the disturbance can be modeled as multiplicative and additive Gaussian perturbations to the transmitted signal. The results showed that the error rate for the optimum detector continues to decrease rapidly for increasing SNR (at least for error rates between 1.0 and 10^{-4}). However, the error rates for conventional coherent and incoherent receivers were seen to saturate, for large SNR, at levels which depend on the strength of the multipath interference. Another very interesting result was that the superior performance of the optimum detector does not require perfect phase references for the carrier demodulation.

It has also been shown that MSK, a coherent signalling scheme presently used in a continental air-ground data-link, can be used in the presence of strong multipath. Now, the simulated multipath process was totally diffuse, of a strength and bandwidth comparable to that encountered over an ocean surface at L-band for the aircraft-satellite geometry.⁸ Thus, it appears that the same signalling scheme which is used over land may also be usable over the ocean, even in the presence of severe multipath.

The significance of the above conclusions depends, of course, on whether practical receivers can be implemented with error rates approaching the bounds given by the simulation. Practical implementation, in turn, depends on solving the real-time estimation problem for the statistics of the multiplicative (multipath) process. The authors are already in possession of partial solutions to this problem. It can be stated, now, that practical solutions to the statistics estimation problem exist. Proof of this statement will be left to a future paper.

⁸ R.W. Sutton, E.H. Schroeder, A.D. Thompson, and S.G. Wilson, "Satellite-Aircraft Multipath and Ranging Experiment Results at L-Band," IEEE TRANS. ON COHM., vol. COM-21, no. 5, pp. 639-647, May, 1973.

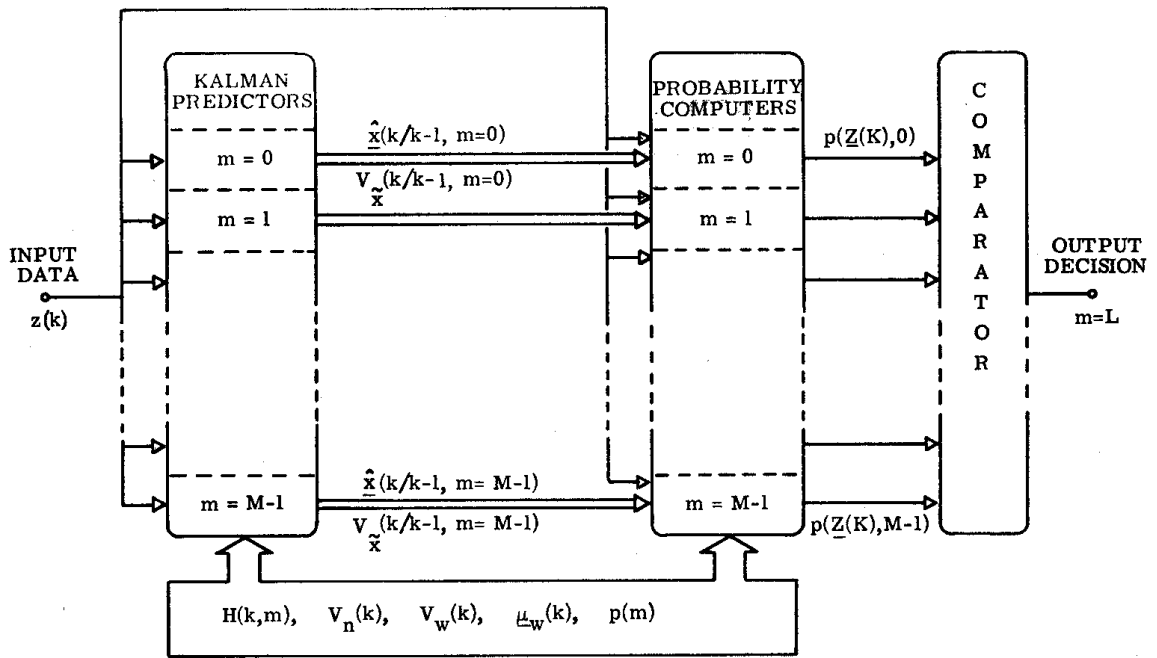


Figure 1. Receiver Structure.

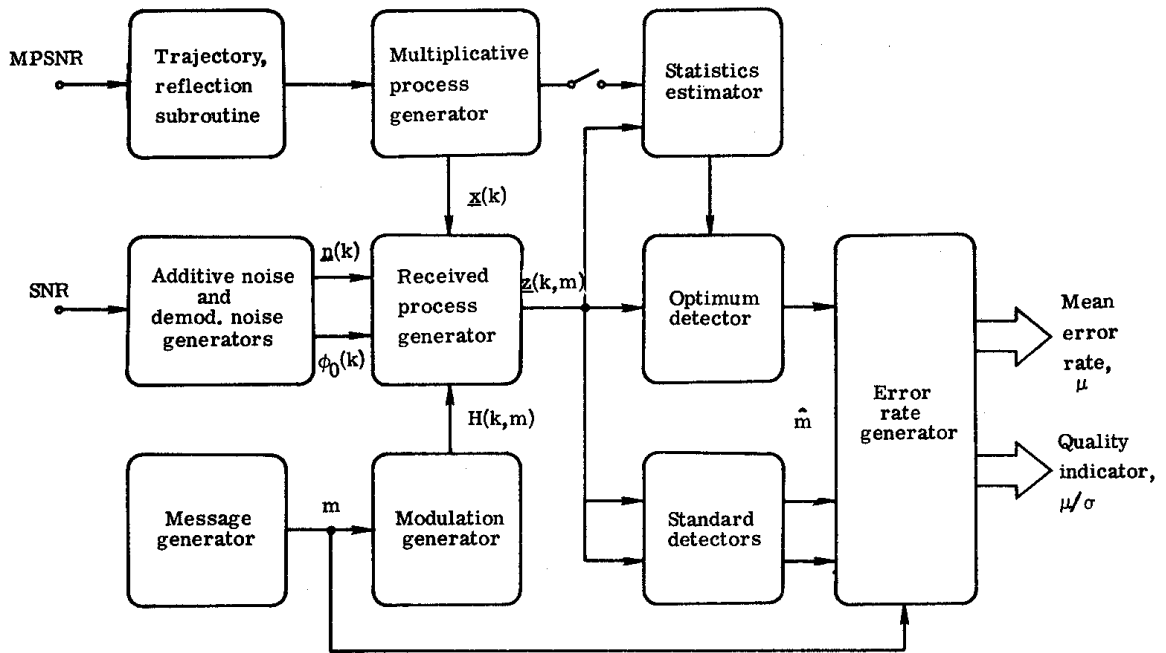


Figure 2. Simulation Block Diagram.

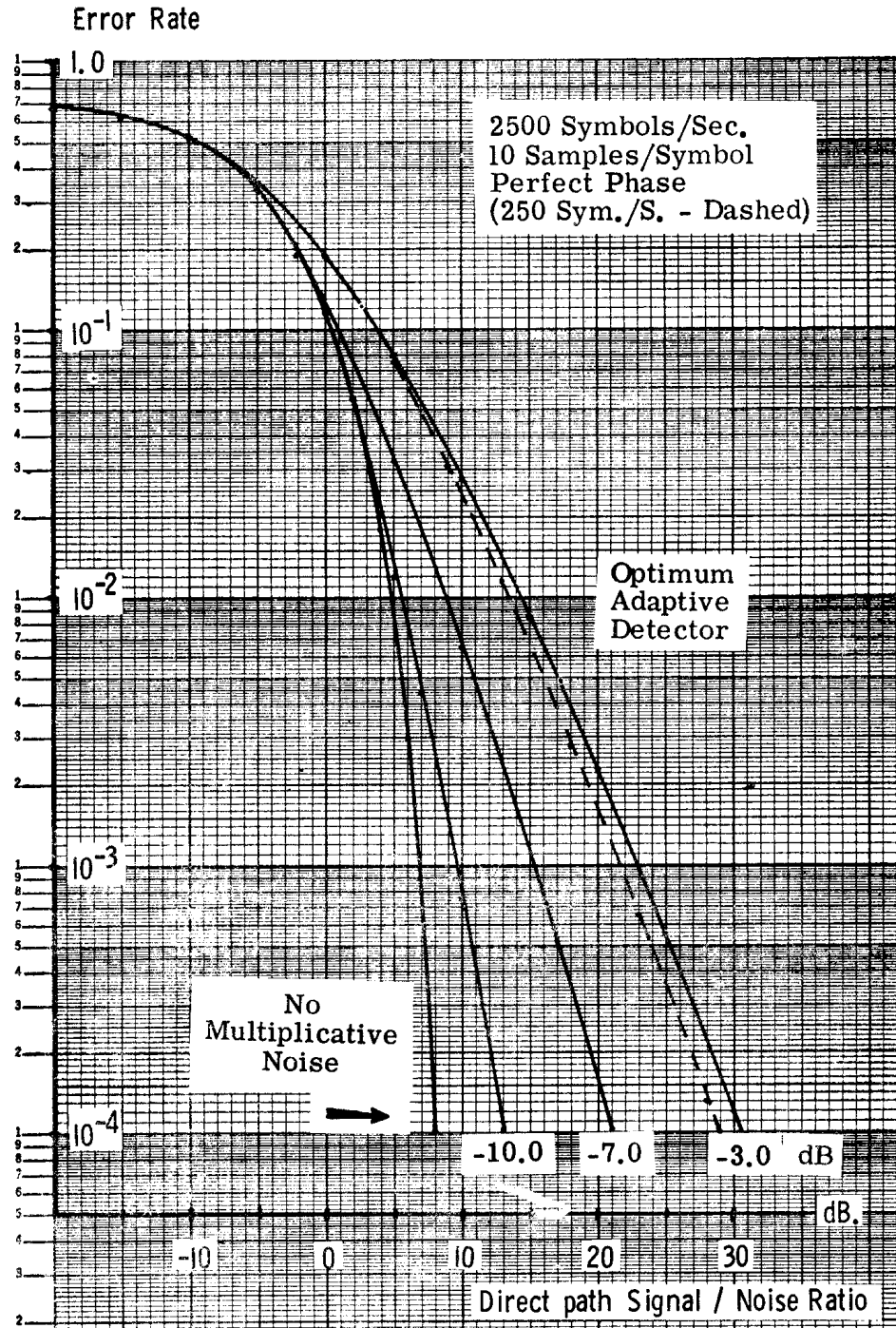


Figure 3. Optimum Detector Performance.

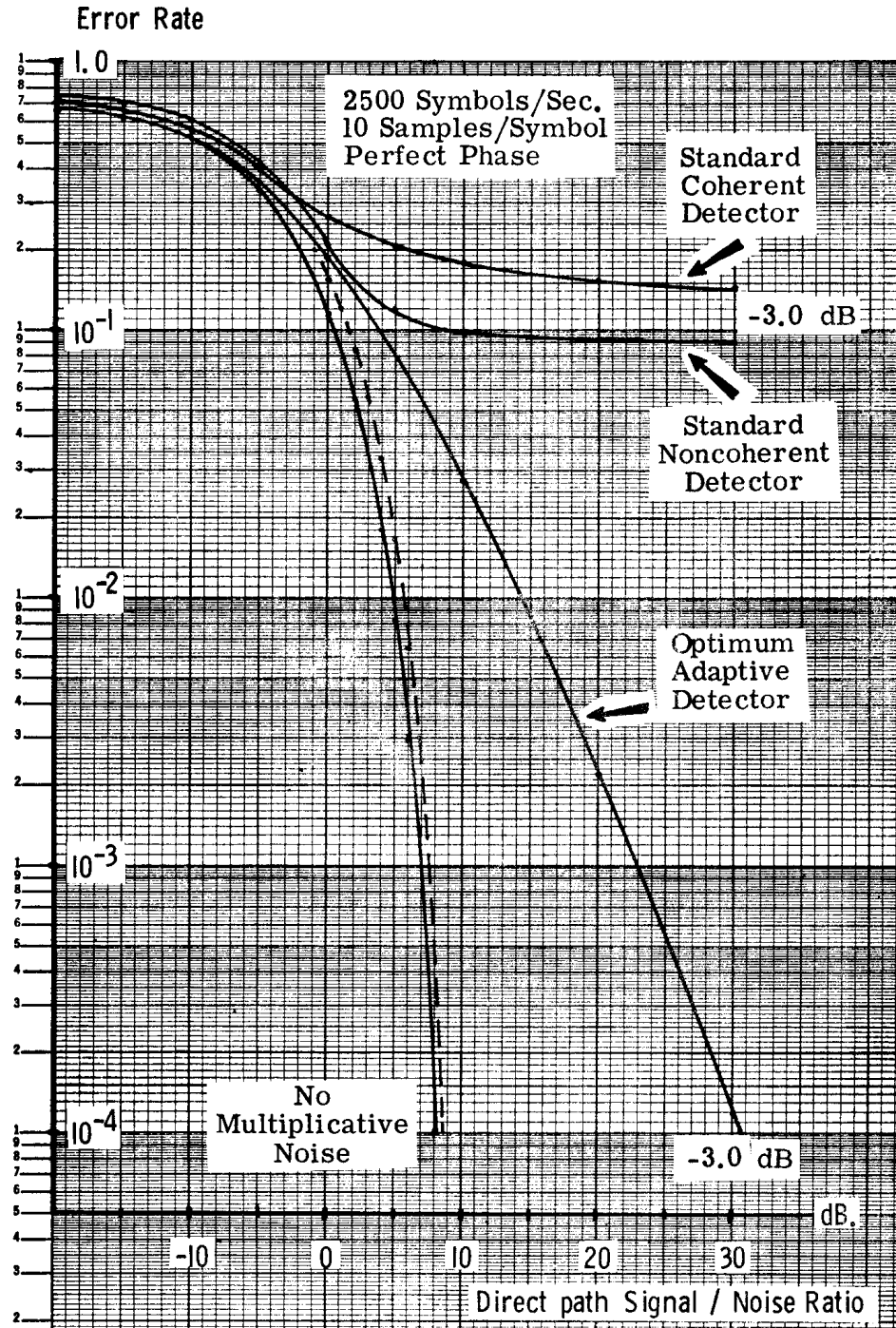


Figure 4. Optimum Detector/Conventional Detector Comparison.

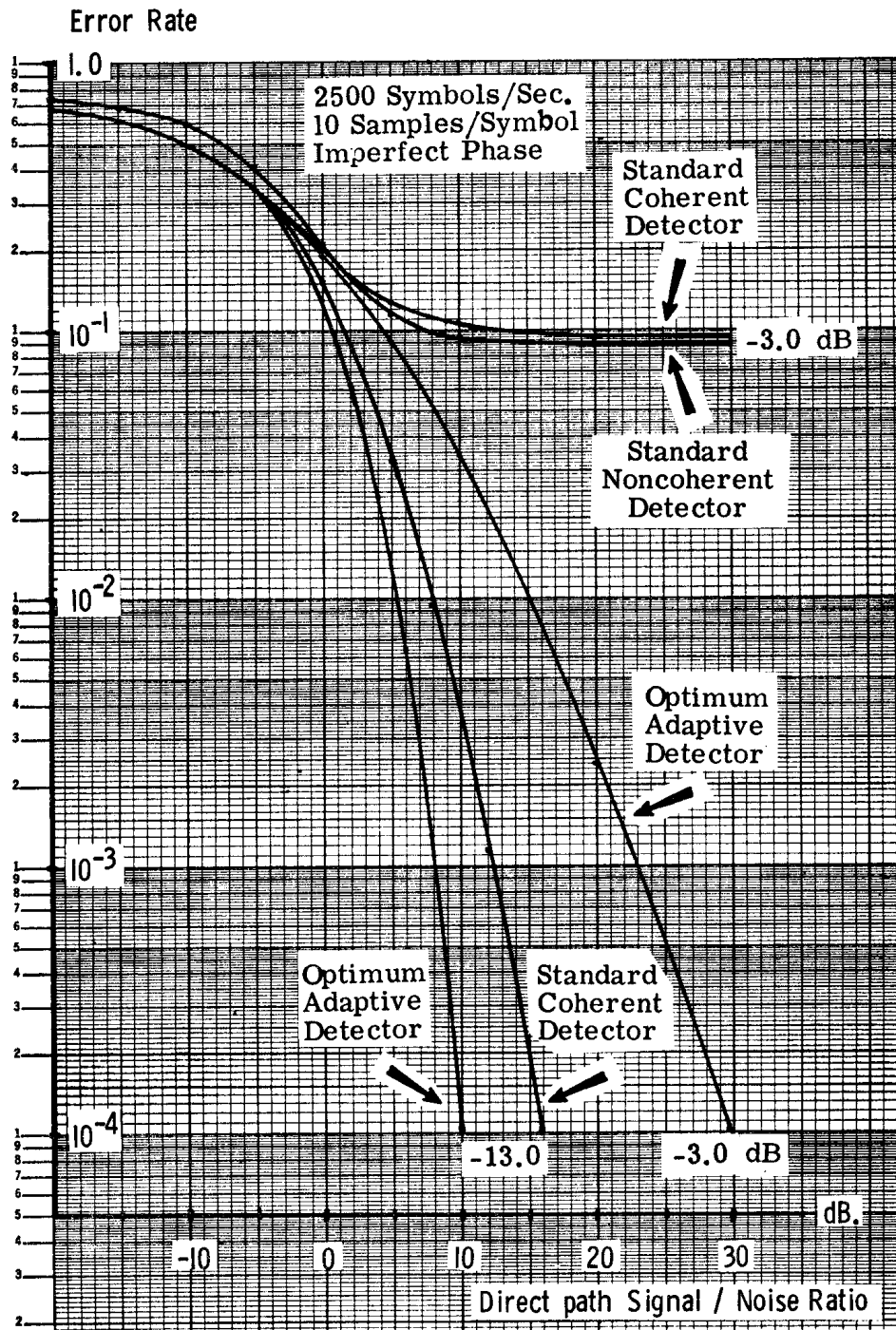


Figure 5. Performance With imperfect Phase Reference.